Supporting Information

Bifunctional Na-Deficient Strategy Induced Pure Phase $Na_{4-x}Fe_3(PO_4)_2P_2O_7$ Cathode with High Capacity for Sodium-Ion Batteries

Rongze Ma,[a] Jiaqi Meng,[c] Xuping Su,[b] Qidi Wang,[d] Ze Li,[b] Qihang Zeng,[a] Yawei Jing,[a, *] Long Li,[b, *] and Shujiang Ding. [b, c, d, *]

a. Shaanxi Coal and Chemical Industry Technology Research Institute Co., Ltd., Xi'an, Shaanxi 710100, P. R. China.

b. School of Chemistry, Xi'an Key Laboratory of Sustainable Energy Materials Chemistry, State Key Laboratory for Mechanical Behavior of Materials, Xi'an Jiaotong University, Xi'an, Shaanxi 710049, P. R. China.

c. National innovation Platform (Center) for industry-Education integration of Energy Storage Technology, Xi'an Jiaotong University, Xi'an, Shaanxi 710049, P. R. China.

d. School of Future Technology, Xi'an Jiaotong University, Xi'an, Shaanxi 710049, P. R. China.

* These authors are co-corresponding authors.

Experimental section

Materials Synthesis.

All reagents used were of analytically pure grade and purchased from Aladdin Reagent (Shanghai) Co., Ltd. $Na_4Fe_3(PO_4)_2(P_2O_7)$ material was prepared by a simple solid-state method. In a typical process, 0.3 mol of $FeC_2O_4·2H_2O$, 0.2 mol of Na_2HPO_4, 0.2 mol of $NH_4H_2PO_4$, 0.04 mol of citric acid and 5wt% of polyethylene glycol (PEG) were added to deionized water and stirred, then poured into ball milling jar for thorough mixing and particle size reduction at 400 rpm for 10 h. Subsequently, spray drying was performed at 240 °C under air conditions to obtain a precursor powder, which was annealed at 500 °C for 10 hours under an argon atmosphere to obtain a spherical carbon-coated $Na_4Fe_3(PO_4)_2(P_2O_7)$ (denoted as NFPP-0). By adjusting the ratio of Na_2HPO_4 to $NH_4H_2PO_4$ in the raw materials, different degrees of Na-deficient $Na_{4-x}Fe_3(PO_4)_2(P_2O_7)$ were prepared (denoted as NFPP-ND). Since the specific adjustments involve the company's (Shaanxi Coal and Chemical Industry Technology Research Institute Co., Ltd.) commercial secrets, they are not detailed here. If readers are interested in these parameters, please consult the corresponding authors.

Material Characterization.

The sample was characterized using an X-ray diffractometer (XRD, Cu Kα, D8 Advance), and the XRD refinement was completed with the GSAS software. X-ray photoelectron spectroscopy (XPS) was employed to characterize the composition of the material and the valence state of the elements. Scanning electron microscopy (SEM, EM-30 plus, COXEM) was used to observe the surface morphology and energy dispersive spectroscopy (EDS). High-resolution transmission electron microscopy (HR-TEM, JEM-1400 Flash) was utilized to detect the microstructure of the sample. A thermogravimetric analyzer (TGA, DTA6300) was used to analyze the carbon content of the sample. Fourier transform infrared spectroscopy (FTIR, T27) was employed to characterize the detailed structural features of the sample.

Electrochemical Measurements.

To prepare the cathode electrode, a slurry with a weight ratio of 7:2:1 of NFPP, super P, and PVDF was thoroughly mixed with an adequate amount of NMP, coated onto a smooth aluminum foil, vacuum-dried, and then punched into circular discs with a diameter of 12 mm. The hard carbon

electrode was composed of hard carbon material, acetylene black, and PVDF in a mass ratio of 8:1:1, which was subsequently punched into circular discs with a diameter of 14 mm. For the coin-type half-cell, the electrolyte used was a solution of 1 M NaPF6 in EC: PC (1:1 volume ratio) + 5wt% FEC. Sodium metal (Sigma-Aldrich, >99%) was used as the counter electrode. Galvanostatic charge/discharge measurements at different current densities were conducted on a Land battery test system ranging from 1.5 V to 4.3 V. Specifically, the nominal capacity at 1 C was designated as 129 mA/g. In terms of the fabrication of coin-type full-cells, all testing procedures and the use of electrolyte were the same as those for the half-cell assembly, except that the hard carbon electrode was used as the counter electrode. For the galvanostatic intermittent titration technique (GITT) experiments, the electrode was charged or discharged at 0.1 C for 20 minutes, followed by a 120-minute rest to reach a steady state. Prior to the GITT experiment, the battery was cycled for two cycles at 0.1 C. Electrochemical impedance spectroscopy (EIS) measurements were performed using an electrochemical workstation (Jiangsu Donghua Analytical Instruments Co., Ltd.) with an amplitude of 5 mV and a frequency range from 0.01 Hz to 100 kHz. Cyclic voltammetry (CV) tests were carried out at scan rates of 0.2~1.0 mV s^{-1} (in increments of 0.2).

Supporting Tables

Table S1. Structural parameters of NFPP-0 determined by the Rietveld refinement.

Reliability factors of Rietveld refinement: R_p=1.85%, R_{wp}=2.42 %, χ^2=1.99

Phase composition: NFPP phase: 86.9%; NFP phase: 13.1%

NFPP phase in NFPP-0 composites：

Cell Parameters	Atom	Position			Occ.
		x	y	z	
	Fe1	0.3333	0.12383	0.52464	1
	Fe2	0.15484	0.63324	0.49326	1
	Fe3	0.24013	0.33549	0.76667	1
	P1	0.3375	0.64733	0.50574	1
	P2	0.20019	0.08231	0.46578	1
	P3	0.5485	0.43546	0.73321	1
	P4	0.44515	0.21168	0.75017	1
	Na1	0.51434	0.78685	0.98456	1
a=18.02703 Å	Na2	0.30938	0.81053	0.67436	1
b=6.54124 Å	Na3	0.4528	0.49461	0.25117	1
c =10.68952 Å	Na4	0.49105	0.77244	0.53506	1
α=β=γ=90.0000	O1	0.19237	0.59141	0.6613	1
Volume=1260.49 Å^3	O2	0.34028	0.42082	0.38687	1
	O3	0.29747	1.09392	0.64462	1
	O4	0.25997	0.62227	0.47622	1
	O5	0.28283	0.22076	0.70238	1
	O6	0.07348	0.0713	0.53338	1
	O7	0.27286	0.10836	0.45328	1
	O8	0.17069	0.29083	0.46972	1
	O9	0.42624	0.47372	0.72007	1
	O10	0.6227	0.34139	0.97737	1
	O11	0.65366	0.34895	0.73968	1

O12	0.57406	0.59561	0.64369	1
O13	0.47969	0.14556	1.06889	1
O14	0.39836	0.13405	0.59479	1
O15	0.45561	0.04319	0.73718	1

Space group：*Pn2$_1$a*

NFP phase in NFPP-0 composites：

Cell Parameters	Atom	Position			Occ.
		x	y	z	
a=9.06515 Å	Fe1	0	0	0	1
b=6.87163 Å	P1	0.16021	0.25	0.45962	1
c =5.00147 Å	Na1	0.42749	0.25	0.58191	1
α=β=γ=90.0000	O1	0.13648	0.06899	0.36917	1
Volume=311.553 Å^3	O2	0.3368	0.25	0.21396	1
	O3	0.11841	0.25	0.6811	1

Space group：*Pnma*

Table S2. Structural parameters of NFPP-ND-1 determined by the Rietveld refinement.

Reliability factors of Rietveld refinement: R_p=1.89%, R_{wp}=2.46 %, χ^2=2.10

NFPP phase in NFPP-ND-1 composites：

Cell Parameters	Atom	Position			Occ.
		x	y	z	
	Fe1	0.33154	0.11876	0.49034	0.984
a=17.89641 Å	Fe2	0.13947	0.61166	0.49182	1.034
b=6.53117Å	Fe3	0.24399	0.35977	0.75669	0.990
c =10.66395Å	P1	0.2939	0.5969	0.50842	1
α=β=γ=90.0000	P2	0.17722	0.12325	0.48948	1
Volume=1246.44 Å^3	P3	0.56567	0.47695	0.73576	1
	P4	0.44782	0.16786	0.73624	1
	Na1	0.49458	0.80133	0.97251	1.0093

Na2	0.31171	0.88331	0.74747	0.9759
Na3	0.37923	0.44859	0.22192	0.9925
Na4	0.47156	0.72958	0.49224	0.8964
O1	0.2303	0.55747	0.52437	1
O2	0.35067	0.44094	0.45913	1
O3	0.36017	0.82753	0.55717	1
O4	0.24536	0.63577	0.35122	1
O5	0.22508	0.09624	0.58302	1
O6	0.14281	-0.06322	0.5403	1
O7	0.23699	-0.01124	0.34238	1
O8	0.12439	0.28086	0.4678	1
O9	0.45481	0.42046	0.73337	1
O10	0.53892	0.57614	0.87059	1
O11	0.62401	0.35449	0.79882	1
O12	0.58722	0.59827	0.59531	1
O13	0.45676	0.08903	0.90541	1
O14	0.35896	0.16402	0.71281	1
O15	0.50267	0.00687	0.65096	1

Space group：*$Pn2_1a$*

Table S3. The charging specific capacity contributed by Na extraction at different positions.

Samples	Na3+Na1		Na4	
	charge slopes (mAh/g)	**charge voltage plateaus (mAh/g)**	**charge slopes (mAh/g)**	**charge voltage plateaus (mAh/g)**
NFPP	3.8	41	7.3	57.6
NFPP-ND-1	4.9	50.4	7.7	64.3
NFPP-ND-2	4.7	45.0	7.6	60.6

Table S4. The diffusion coefficient of sodium ions calculated for NFPP-0 electrode by equation S5.

Peak*x*	NFPP-0 ($cm^2\ s^{-1}$)	NFPP-ND-1 ($cm^2\ s^{-1}$)
Peak1	2.83×10^{-10}	2.98×10^{-10}
Peak2	2.96×10^{-10}	3.01×10^{-10}
Peak3	2.28×10^{-10}	2.49×10^{-10}
Peak4	8.60×10^{-11}	1.21×10^{-10}

Table S5. The charge transfer resistance (R_{ct}) and inner impedance of cell from EIS test.

Samples	R_{ct} (Ohm)	R_c(Ohm)	R_s (Ohm)
NFPP-0-initial	1851.9	20.74	1.316
NFPP-ND-1-initial	1235.2	18.67	1.588
NFPP-0-1st	63.44	15.59	1.717
NFPP-ND-1-1st	62.17	14.43	2.218
NFPP-0-200th	539.8	15.21	1.876
NFPP-ND-1-200th	296.1	14.76	2.148

Table S6. The Comparison of the results in this study with previously reported performance of Fe-based cathode for SIBs.

Sample	Capacity	Cycling stability	Ref.
NFPP-HE	122 mAh g^{-1} at 0.1 C; 100 mAh g^{-1} at 10 C; 85.2 mAh g^{-1} at 50 C	94.3% after 500 cycles at 1C; 82.3% after 1500 cycles at 10 C	1
NFPP-Mg5%	104 mAh g^{-1} at 0.05 A g^{-1}; 40 mAh g^{-1} at 20 A g^{-1}	80.8% after 14000 cycles at 5 A g^{-1}	2
$Na_4Fe_{2.91}(PO_4)_2P_2O_7$	110.9 mAh g^{-1} at 0.2 C; 65 mAh g^{-1} at 50 C; 52 mAh g^{-1} at 100 C	No deacy after 10000 cycles at 50 C	3
$Na_{3.4}Fe_{2.4}(PO_4)_{1.4}P_2O_7$	110.8 mAh g^{-1} at 0.1 C; 50.5 mAh g^{-1} at 100 C	83.1% after 14000 cycles at 20 C	4

NFPP-Mn-F	121 mAh g^{-1} at 0.1 C; 104.9 mAh g^{-1} at 5 C	88.5% after 1000 cycles at 1 C	5
NFPP-nanofibers	136 mAh g^{-1} at 0.1 C; 85 mAh g^{-1} at 5 C	95.2% after 1200 cycles at 5 C; 79.6% after 10000 cycles at 10 C	6
$Na_4Fe_{2.82}Ni_{0.18}(PO_4)_2P_2O_7$@C-N	128.4 mAh g^{-1} at 0.2 C; 62.5 mAh g^{-1} at 50 C	83% after 3000 cycles at 10 C	7
$Na_4Fe_{2.9}Al_{0.1}(PO_4)_2P_2O_7$	114.5 mAh g^{-1} at 0.1 C	98.5% after 200 cycles at 0.5 C; 85.1% after 10000 cycles at 50 C	8
$Na_{3.12}Fe_{2.44}(P_2O_7)_2$/r-GO	116.4 mAh g^{-1} at 0.2 C; 72.3 mAh g^{-1} at 20 C	88.82% after 5000 cycles at 0.1 C	9
M-Na_2FePO_4	145 mAh g^{-1} at 0.2 C; 61 mAh g^{-1} at 50 C	89% after 6300 cycles at 5 C	10
O-Na_2FePO_4	111 mAh g^{-1} at 0.1 C; 46 mAh g^{-1} at 2 C	90% after 240 cycles at 0.1 C	11
$Na_2FeP_2O_7$	95.2 mAh g^{-1} at 0.1 C; 75.2 mAh g^{-1} at 5 C	95.3% after 500 cycles at 5 C	12
NFPP-ND-1	**127.2 mAh g^{-1} at 0.1 C; 102.6 mAh g^{-1} at 10 C**	**100% after 450 cycles at 1 C; 99.16% after 300 cycles at 5 C**	**This work**

Table S7. The comparison electrochemical performance of NFPP-ND-1//HC full cell with recently reports.

Full-cell (cathode//anode)	Capacity	Cycling stability	Ref.
NFPP-Mg5%//HC	77.5 mAh g^{-1} at 500 mA g^{-1}	64.5% after 200 cycles at 500 mA g^{-1}	2
$Na_4Fe_{2.91}(PO_4)_2P_2O_7$//HC	0.35Ah at 0.1 C	87.4% after 10000 cycles at 1 C	3

$Na_{3.4}Fe_{2.4}(PO_4)_{1.4}P_2O_7$//HC	93.8 mAh g^{-1} at 10 mA g^{-1}	100% after 100 cycles at 50 mA g^{-1}	4
NFPP-Mn-F//HC	107.8 mAh g^{-1} at 0.2 C;	78.8% after 100 cycles at 1 C	5
Na4Fe3(PO_4)2(P_2O_7)//HC	124 mAh g^{-1} at 0.2 C; 30.4 mAh g^{-1} at 5 C	73.2% after 180 cycles at 1 C	6
N4FP-5% N2FP//HC	80.2 mAh g^{-1} at 0.1 C; 50 mAh g^{-1} at 5 C	88% after 200 cycles at 2 C	13
$Na_4Fe_{2.9}Al_{0.1}(PO_4)_2P_2O_7$//HC	102.7 mAh g^{-1} at 0.1 C; 92.3 mAh g^{-1} at 5 C	No deacy after 150 cycles at 2 C	8
NFPP-ND-1//HC	**108 mAh g^{-1} at 0.1 C; 79.8 mAh g^{-1} at 5 C**	**96.5% after 150 cycles at 1 C**	**This work**

Supporting Figures

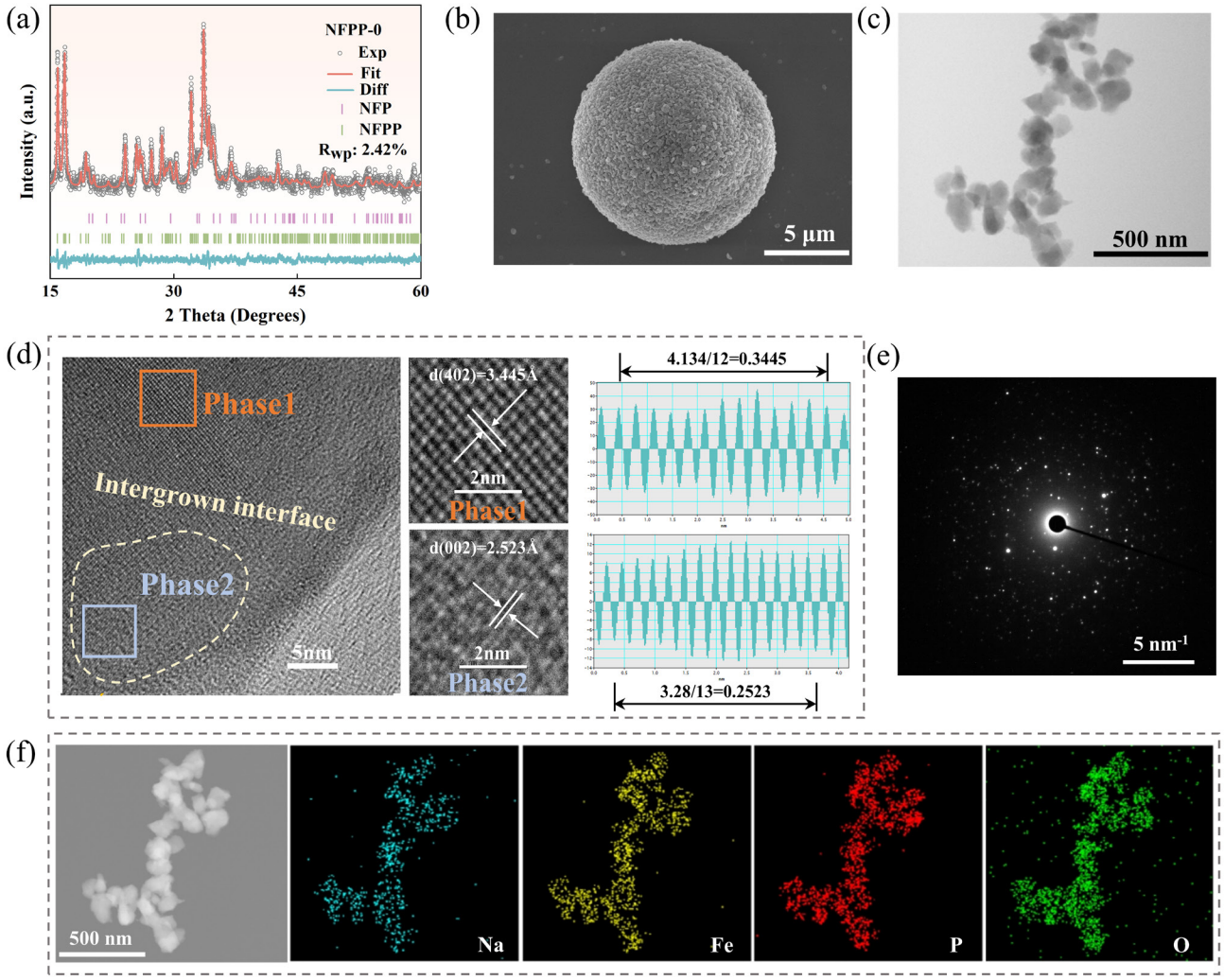

Fig. S1 Characterizations of the as-prepared samples. a) Rietveld refinements of NFPP-0. b) SEM image of NFPP-0. c) TEM images of NFPP-0. d) High magnification TEM image and inverse FFT of NFPP-0. e) SAED pattern of NFPP-0. f) EDS elemental mappings of NFPP-0.

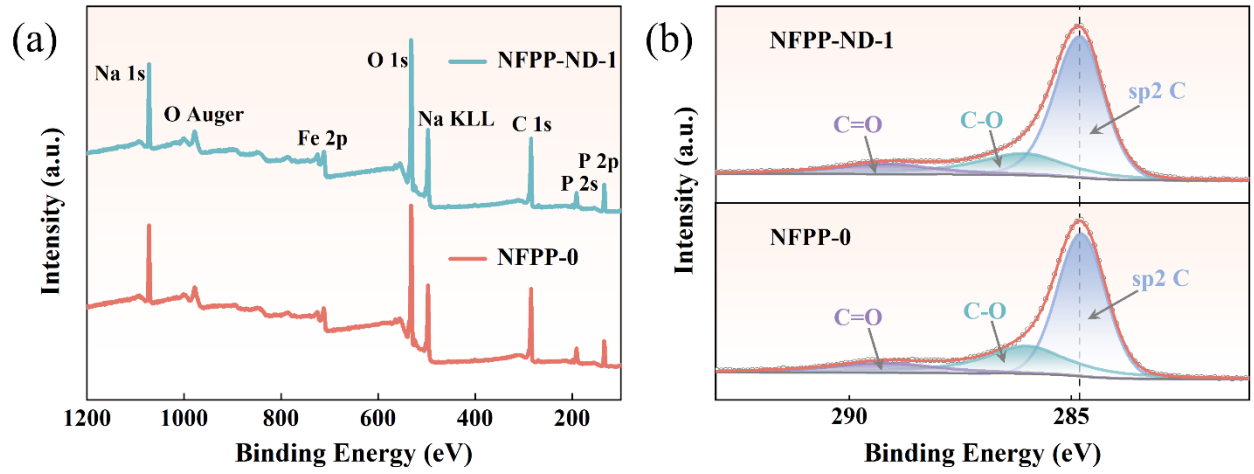

Fig. S2 a) XPS spectra and b) C 1s spectrum of NFPP-0 and NFPP-ND-1 samples.

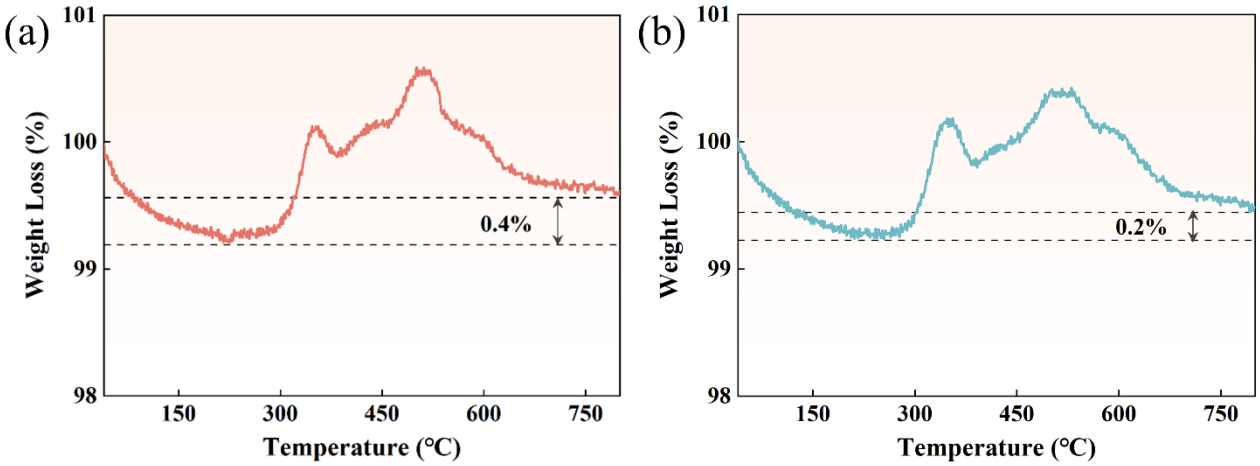

Fig S3 Thermogravimetric analysis in air atmosphere of the two samples. a) NFPP-0. b) NFPP-ND-1.

The speculated reaction of NFPP during annealing in the air is described as the following equation[2]:

$$Na_4Fe_3(PO_4)_2P_2O_7+3/4O_2=4/3Na_3Fe_2(PO_4)_3+1/6Fe_2O_3 \quad \textbf{(S1)}$$

All the calculation of carbon content were relied on the law of conservation of mass. Thus, the equation is:

$$\textbf{the content of carbon (\%)} = x + y \times [3/4MO_2 \div (4/3MNa_3Fe_2(PO_4)_3+1/6MFe_2O_3)] \quad \textbf{(S2)}$$

where x is the percentage of weight loss after heating is completed, and y is the percentage of weight ratio after heating to 250°C.

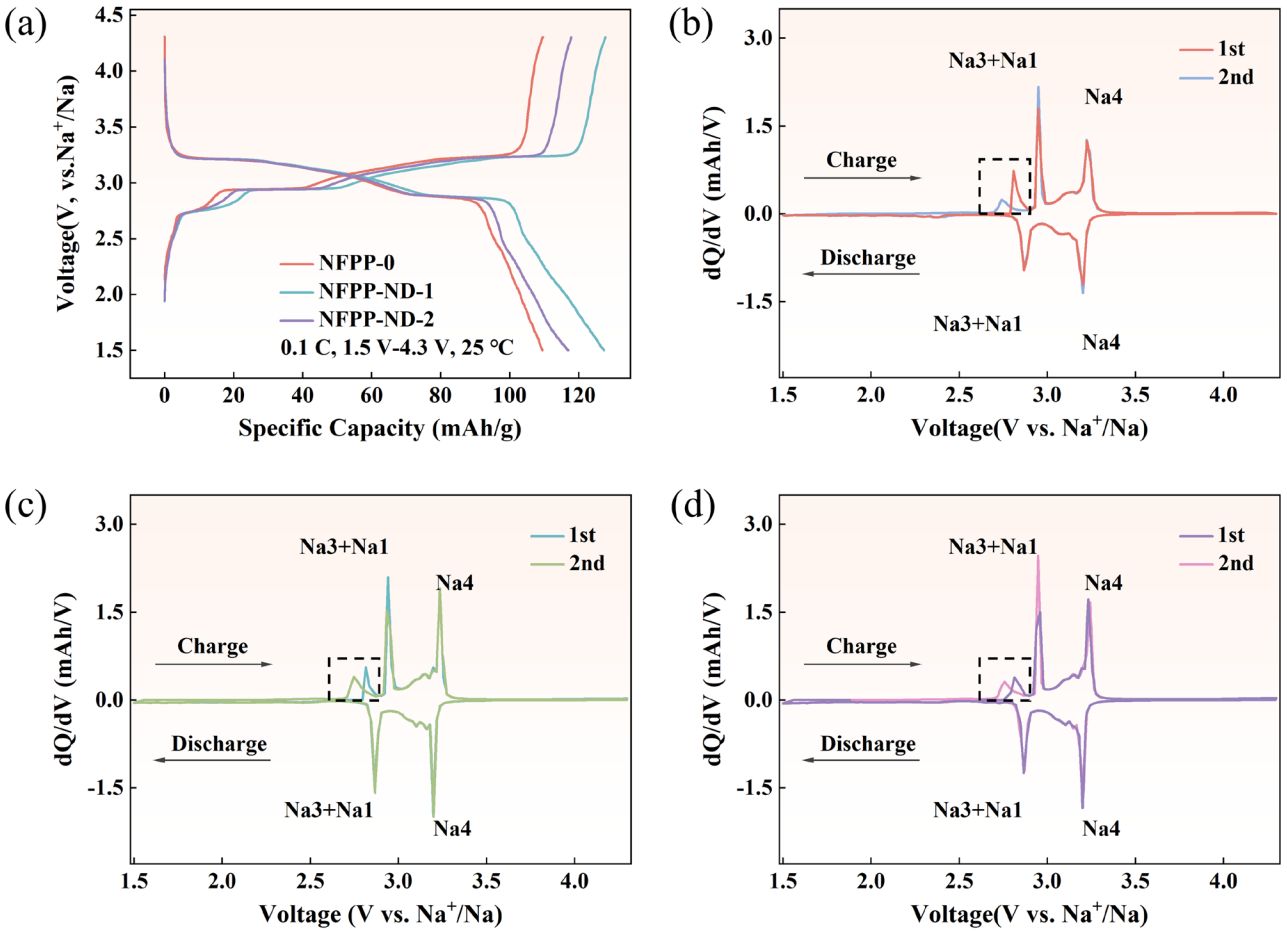

Fig. S4 a) The charge/discharge profiles of the second cycle at 0.1 C. Initial two dQ/dV curves of the three electrodes at 0.1 C. b) NFPP-0. c) NFPP-ND-1. d) NFPP-ND-2.

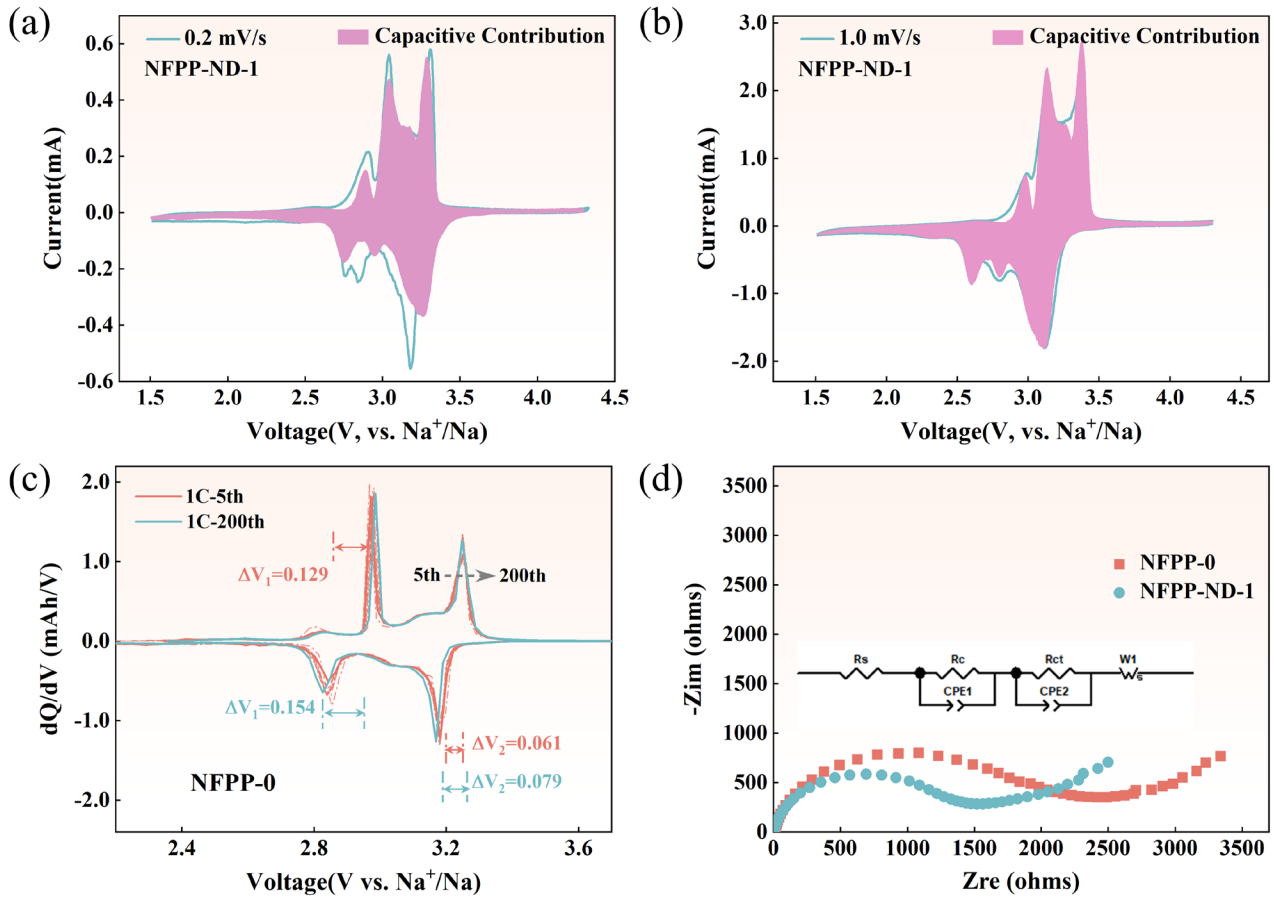

Fig. S5 Fitted pseudocapacitive contribution (light purple area) of NFPP-ND-1 electrode at scan rates of a) 0.2 mV/s and b) 1 mV/s. c) The charge/discharge differential capacity versus voltage profiles (dQ/dV) during 200 cycling process of NFPP-0. d) The initial EIS spectra of NFPP-0 and NFPP-ND-1 electrodes and the inset is the equivalent circuit.

The charge-storage mechanism involves two important components: Faradaic contribution including diffusion-controlled reaction and pseudocapacitance, and non-Faradaic contribution of doublelayer capacitance. According to the relationship between the response current (i) under a certain potential (V) and the sweep rate (v):[4, 7]

$$i = av^b \quad \text{(S3)}$$

$$\log i = b \times \log v + \log a \quad \text{(S4)}$$

where the b-value is determined by the ion storage mechanism and can be calculated by slope of the log(i)−log(v) plot. To be more specific, the b-value of 0.5 means a completely diffusion-controlled process, whereas a b-value of 1.0 indicates a faradaic contribution.

The diffusion coefficient of sodium ion within the electrode can be calculated based on the following

formula:

$$\boldsymbol{I_p = 2.69 \times 10^5 n^{3/2} A D_{Na^+}^{1/2} C_{Na^+}^{*} v^{1/2}} \quad \textbf{(S5)}$$

where I_p is the peak current (A), n is the charge-transfer number, A is the contact area between working electrode and electrolyte, D_{Na^+} is the diffusion coefficient of sodium ion, C_{Na^+} is the bulk concentration of sodium ion in electrode, and v is the scan rate.

Quantitatively, these two components can be discriminated by evaluating the current response (i) at a fixed potential (V) via the equation:

$$\boldsymbol{i(V) = k1(V)v + k2(V)v^{1/2}} \quad \textbf{(S6)}$$

where k1(V)v and k2(V)$v^{1/2}$ originate from the capacitive and diffusion-controlled effects, respectively.

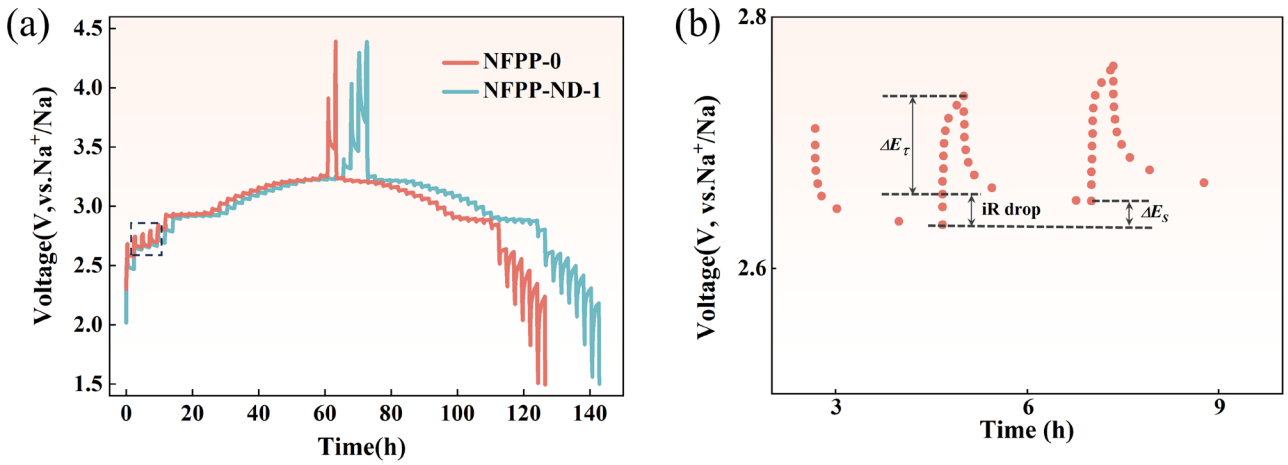

Fig. S6 a) GITT curves of NFPP-0 and NFPP-ND-1 electrodes. b) Enlarged GITT curve of NFPP-0 electrode.

The galvanostatic intermittent titration technique (GITT) test was carried out by a galvanostatic charge−discharge system (Neware) at room temperature. The electrode was charged or discharged at 0.1C (1 C = 129 mAg^{-1}) for 20 min and then relaxed for 120 min to reach a steady state. The above-mentioned procedure was repeatedly conducted in the range 1.5−4.3 V.

The equation for D_{Na^+} is as follows:[1]

$$\boldsymbol{D_{Na+}} = \frac{4L^2}{\pi\tau}\left(\frac{\Delta E_S}{\Delta E_\tau}\right)^2 \qquad (\tau \ll L^2/D_{Na+}) \qquad \textbf{(S7)}$$

Where L is the effective thickness of the electrode material, τ is the pulse time, π is 3.15, ΔE_S is the open circuit potential difference between two adjacent pulses, and $\Delta E\tau$ is the change of potential caused by an impulse.

References

1. X. C. Ge, H. X. Li, J. Li, C. H. Guan, X. Wang, L. He, S. M. Li, Y. Q. Lai and Z. Zhang, *Small*, 2023, **19**, 10.
2. F. Xiong, J. Li, C. Zuo, X. Zhang, S. Tan, Y. Jiang, Q. An, P. K. Chu and L. Mai, *Adv. Funct. Mater.*, 2023, **33**, 2211257.
3. A. Zhao, T. C. Yuan, P. Li, C. Y. Liu, H. J. Cong, X. J. Pu, Z. X. Chen, X. P. Ai, H. X. Yang and Y. L. Cao, *Nano Energy*, 2022, **91**, 9.
4. Z. Fan, W. Song, N. Yang, C. Lou, R. Tian, W. Hua, M. Tang and F. Du, *Angew. Chem. Int. Ed.*, 2024, **63**.
5. Y. K. Xi, X. X. Wang, H. Wang, M. J. Wang, G. J. Wang, J. Q. Peng, N. J. Hou, X. Huang, Y. Y. Cao, Z. H. Yang, D. Z. Liu, X. H. Pu, G. Q. Cao, R. X. Duan, W. B. Li, J. J. Wang, K. Zhang, K. H. Xu, J. J. Zhang and X. F. Li, *Adv. Funct. Mater.*, 2024, **34**, 11.
6. W. Ren, M. Qin, Y. Zhou, H. Zhou, J. Zhu, J. Pan, J. Zhou, X. Cao and S. Liang, *Energy Storage Mater.*, 2023, **54**, 776-783.
7. W. B. Fei, Y. Wang, X. P. Zhang, J. X. Zhang, S. X. Lu, K. X. Rao, K. Y. Sun, M. T. Deng, Y. X. Liu, Q. Q. Li, L. Wu and Y. L. Sui, *Chem. Eng. J.*, 2024, **493**, 11.
8. J. Gao, J. Zeng, W. Jian, Y. Mei, L. Ni, H. Wang, K. Wang, X. Hu, W. Deng, G. Zou, H. Hou and X. Ji, *Sci. Bull.*, 2024, **69**, 772-783.
9. B. Liu, Y. Zou, S. Chen, H. Zhang, J. Sun, X. She and D. Yang, *Chem. Eng. J.*, 2019, **365**, 325-333.
10. Y. Liu, N. Zhang, F. Wang, X. Liu, L. Jiao and L.-Z. Fan, *Adv. Funct. Mater.*, 2018, **28**, 1801917.
11. Y. Fang, Q. Liu, L. Xiao, X. Ai, H. Yang and Y. Cao, *ACS Appl. Mater. Interfaces*, 2015, **7**, 17977-17984.
12. L. Zhou, H. Yu, B. Zhou, J. Yu, L. Chen and H. Jiang, *Adv. Energy Sustainability Res.*, 2024, **5**, 2400120.
13. Z. Liu, Y. Cao, H. Zhang, J. Xu, N. Wang, D. Zhao, X. Li, Y. Liu and J. Zhang, *ACS Sustain. Chem. Eng.*, 2024, **12**, 1132-1141.